Supporting Information

Control of exposed crystal planes of CeO_2 enhances electrocatalytic nitrate reduction

Fei Wang[1,2,#], Dan Li[1,#], Jian Mao[1]

[1]College of Materials Science and Engineering, Sichuan University, Chengdu 610065, Sichuan, China.
[2]Faculty of Materials Science and Engineering, Kunming University of Science and Technology, Kunming 650093, Yunnan, China.
[#]Authors contributed equally to this work.

Correspondence to: Prof. Jian Mao, College of Materials Science and Engineering, Sichuan University, No.24 South Section 1, Yihuan Road, Chengdu 610065, Sichuan, China. E-mail: maojian@scu.edu.cn; Prof. Fei Wang, Faculty of Materials Science and Engineering, Kunming University of Science and Technology, No. 727 Jingming South Road, Chenggong District, Kunming 650093, Yunnan, China. E-mail: echo1994wf@foxmail.com

1. Determination of ammonia-N

The determination of ammonia-N was performed using a modified indophenol blue spectrophotometry method.[1] Initially, a specific volume of electrolyte solution was extracted from the cathodic electrolytic cell and diluted to 2 mL. Subsequently, 2 mL of a 1 M NaOH solution containing 5 wt% salicylic acid and 5 wt% sodium citrate was added to the diluted solution. Additionally, 50 μL of a 5.5 wt% NaClO solution and 0.2 mL of a 1.0 wt% $C_5FeN_6Na_2O$ solution were introduced. The mixture was thoroughly shaken and allowed to stand at room temperature for 2 hours to undergo the necessary reactions. Following the reaction period, the absorption spectrum of the resulting mixture was measured using a UV-visible spectrophotometer within the wavelength range of 550-750 nm. The concentration of ammonia-N was determined by analyzing the absorbance at 655 nm. To establish the calibration curve, a series of standard NH_4Cl solutions (0, 0.25, 0.5, 1.0, 1.5 and 2 mg L^{-1}) were prepared (NH_4Cl crystals were pre-dried at 105 °C for 2 hours to ensure the accuracy of the standard solutions), By plotting the concentration of the NH_4Cl solutions against their corresponding absorbance values at 655 nm, a calibration curve was generated. This curve could then be used to determine the concentration of ammonia-N in the tested samples based on their absorbance readings at 655 nm.

The ammonia yield rate was calculated by the Equation 1:[2]

$$\mathrm{Yield}_{NH_3} = (c_{NH_4^+} \times V) / (M_{NH_4^+} \times t \times m) \quad (1)$$

The FE of NRA was calculated by the Equation 2:

$$\mathrm{FE}_{NH_3} = (8F \times c_{NH_4^+} \times V) / (M_{NH_4^+} \times Q) \quad (2)$$

Where $c_{NH_4^+}$ is the concentration of NH_4^+ calculated via UV-vis, in mg L^{-1}; V is the volume of the electrolyte, t is the reaction time, in h; m is the load mass of the sample on the working electrode, mg; F is Faraday's constant, 96485 C mol^{-1}; Q is the total charge passing through the working electrode.

2. Calculation details

The DFT calculations were carried out utilizing the Perdew-Burke-Ernzerhof (PBE) generalized gradient approximation (GGA) function within the CASTEP code of Materials Studio 2020 (Accelrys Software Inc., U.S.A.), and the plane-wave expansion was employed with a kinetic energy cutoff set to 500 eV, a k-point mesh of 3×3×1 was used.[3-5] The CeO_2 surface model was constructed using a 2×2 supercell, with a vacuum layer thickness set to 15Å.[6] The total energy, force and displacement convergence was set to 1×10^{-5} eV/atom, 0.03 eV $Å^{-1}$, and 0.001 $Å^{-1}$ respectively.[7] And the chemical

reaction considered can be summarized with the reaction equations below.[8-10]

$$* + \mathrm{NO_3^-} \rightarrow * \mathrm{NO_3^-} + e^- \quad (3)$$

$$* NO_3^- + 2H^+ + 2e^- \rightarrow * NO_2 + H_2O \quad (4)$$

$$* NO_2 + 2H^+ + 2e^- \rightarrow * NO + H_2O \quad (5)$$

$$* NO + 2H^+ + 2e^- \rightarrow * N + H_2O \quad (6)$$

$$* N + H^+ + e^- \rightarrow * NH \quad (7)$$

$$* NH + H^+ + e^- \rightarrow * NH_2 \quad (8)$$

$$* NH_2 + H^+ + e^- \rightarrow * NH_3 \quad (9)$$

$$* NH_3 \rightarrow NH_3 + * \quad (10)$$

Where * represents the active site, and the change in free energy of the reaction can be obtained from the following equation:

$$E_{ad} = E_t - E_s - E_m \quad (11)$$

$$\Delta G = E_{ad} + \Delta E_{ZPE} - T\Delta S \quad (12)$$

where E_{ad} is the adsorption energy, E_t is the total energy of the adsorbate-slab system, and E_s is the energy of the clean slab, and E_m is the energy of the isolated adsorbate. ΔE_{ZPE} and $T\Delta S$ represent zero-point energy and entropy, respectively. The zero-point energy and entropy of the free molecule and adsorbate are calculated using vibrational frequencies.

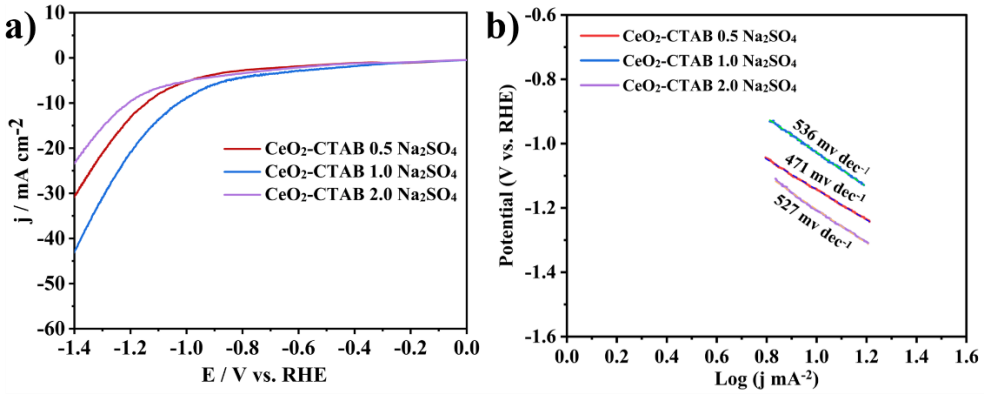

Figure S1. (a) LSV curves of three catalysts in a 0.5 M Na_2SO_4 electrolyte, and (b) the corresponding Tafel slope.

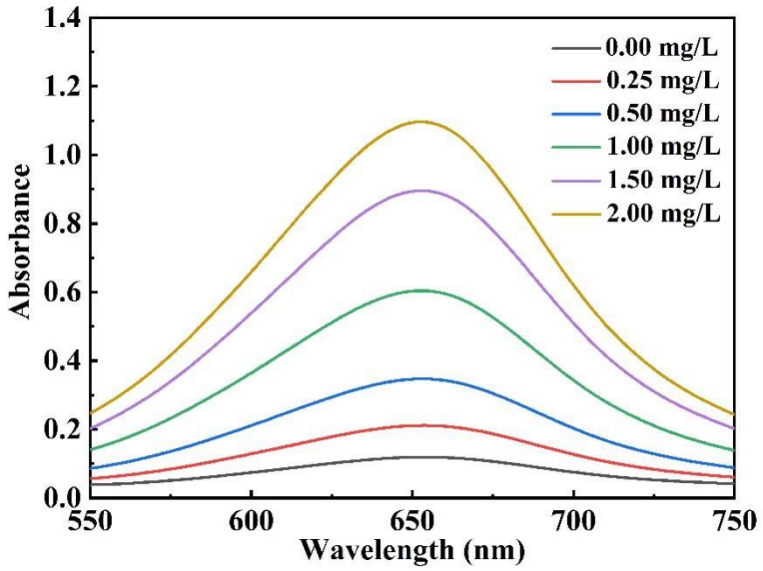

Figure S2. UV-Vis absorption spectra of various NH_4^+ concentrations.

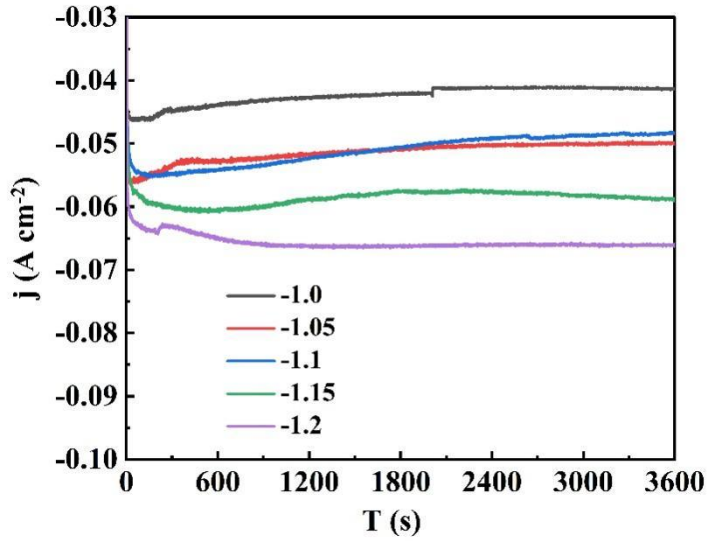

Figure S3. Chronoamperometry curves of CeO_2-CTAB0.5 in a 0.5 M Na_2SO_4 electrolyte with 0.01 M NO_3^-.

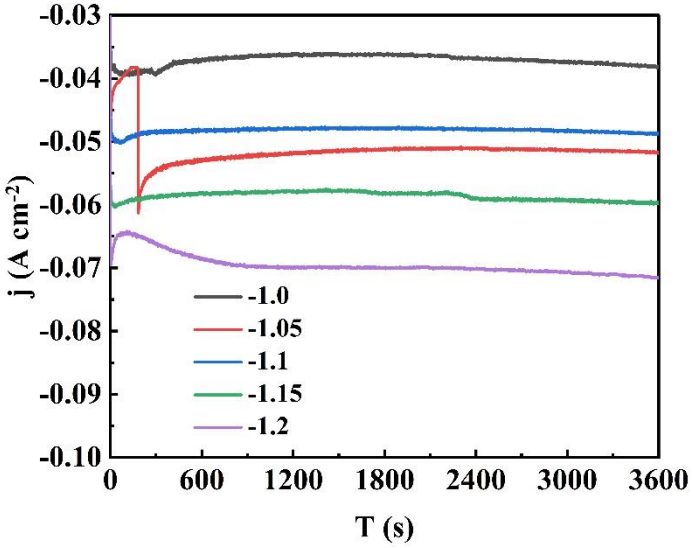

Figure S4. Chronoamperometry curves of CeO_2-CTAB1.0 in a 0.5 M Na_2SO_4 electrolyte with 0.01 M NO_3^-.

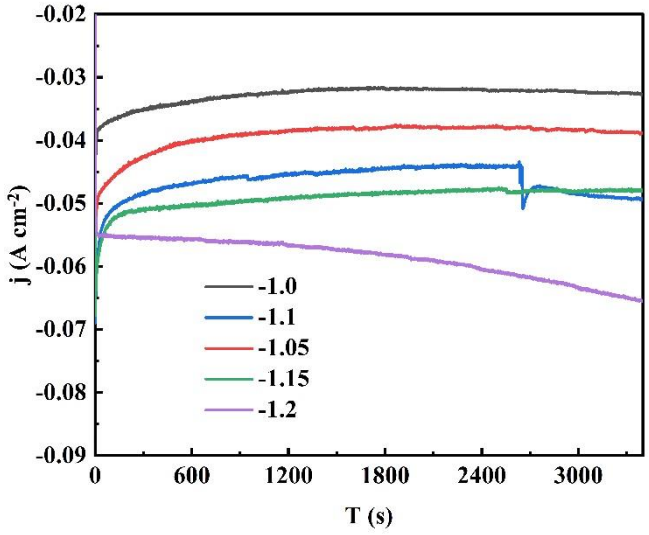

Figure S5. Chronoamperometry curves of CeO_2-CTAB1.0 in a 0.5 M Na_2SO_4 electrolyte with 0.01 M NO_3^-.

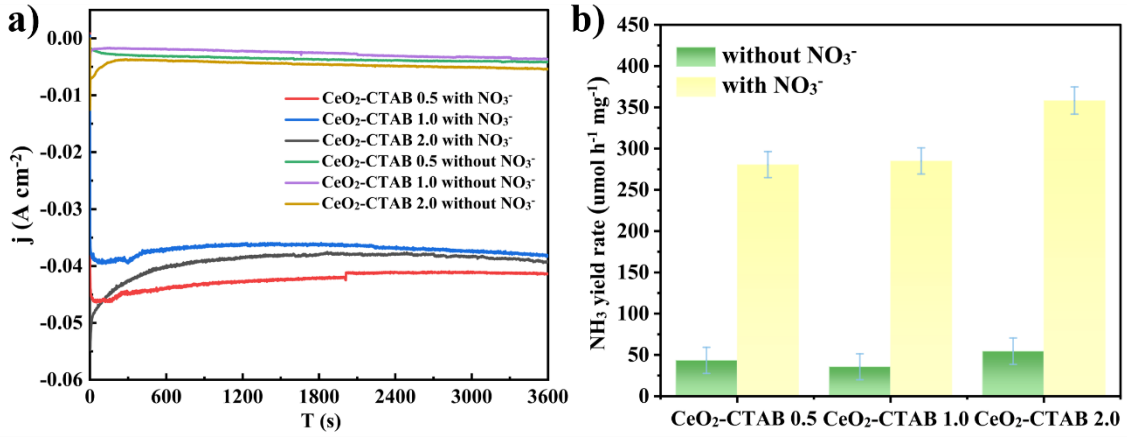

Figure S6. (a) Chronoamperometry curves and (b) $Yield_{NH3}$ of various catalysts in electrolytes with and without NO_3^-.

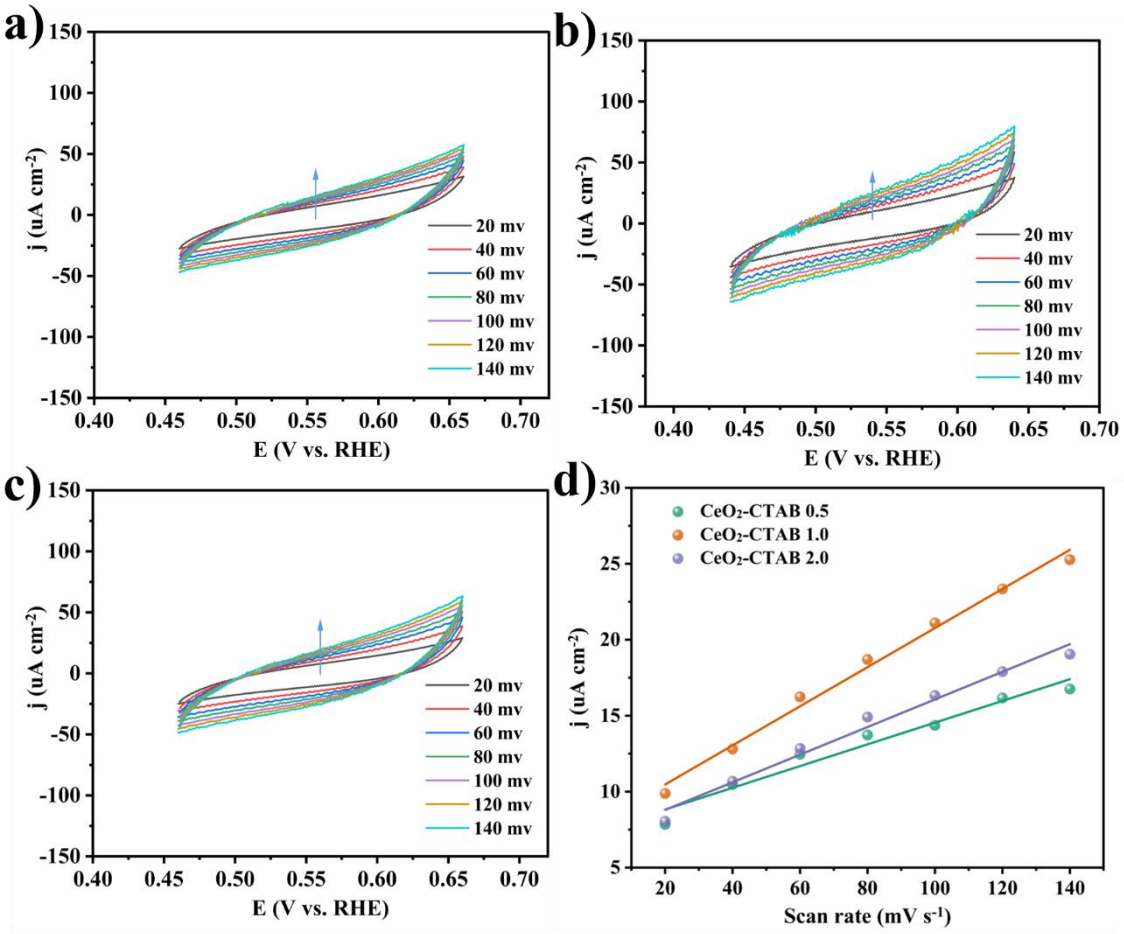

Figure S7. CV curves of (a) CeO_2-CTAB0.5, (b) CeO_2-CTAB1.0 and (c) CeO_2-CTAB2.0 at various scanning rate, and (d) corresponding fitting curves.

Note: The specific capacitance of CeO_2-CTAB0.5, CeO_2-CTAB1.0 and CeO_2-CTAB2.0 are fitted to be 0.07, 0.13 and 0.09 mF cm^{-2} respectively. The specific capacitance for a flat surface is generally found to be in the range of 20-60 μF cm^{-2}. In the following calculations of electrochemical active surface area we assume 40 μF cm^{-2}. Therefore, we calculated the electrochemical active area (ECSA) of each catalyst as follows:

$$A_{ECSA}^{CeO2-CTAB0.5}=\frac{0.07\ mF^{-2}}{40\ uF\ cm^{-2}\ per\ cm_{ECSA}^2}=1.75\ cm_{ECSA}^2$$

$$A_{ECSA}^{CeO2-CTAB1.0}=\frac{0.13\ mF^{-2}}{40\ uF\ cm^{-2}\ per\ cm_{ECSA}^2}=3.25\ cm_{ECSA}^2$$

$$A_{ECSA}^{CeO2-CTAB2.0}=\frac{0.09\ mF^{-2}}{40\ uF\ cm^{-2}\ per\ cm_{ECSA}^2}=2.25\ cm_{ECSA}^2$$

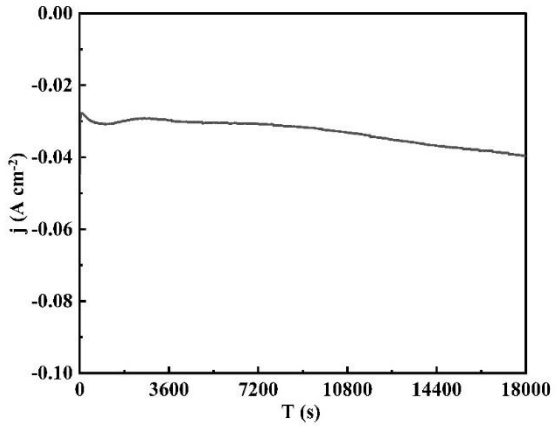

Figure S8. Long-term stability test of CeO2-CTAB2.0.

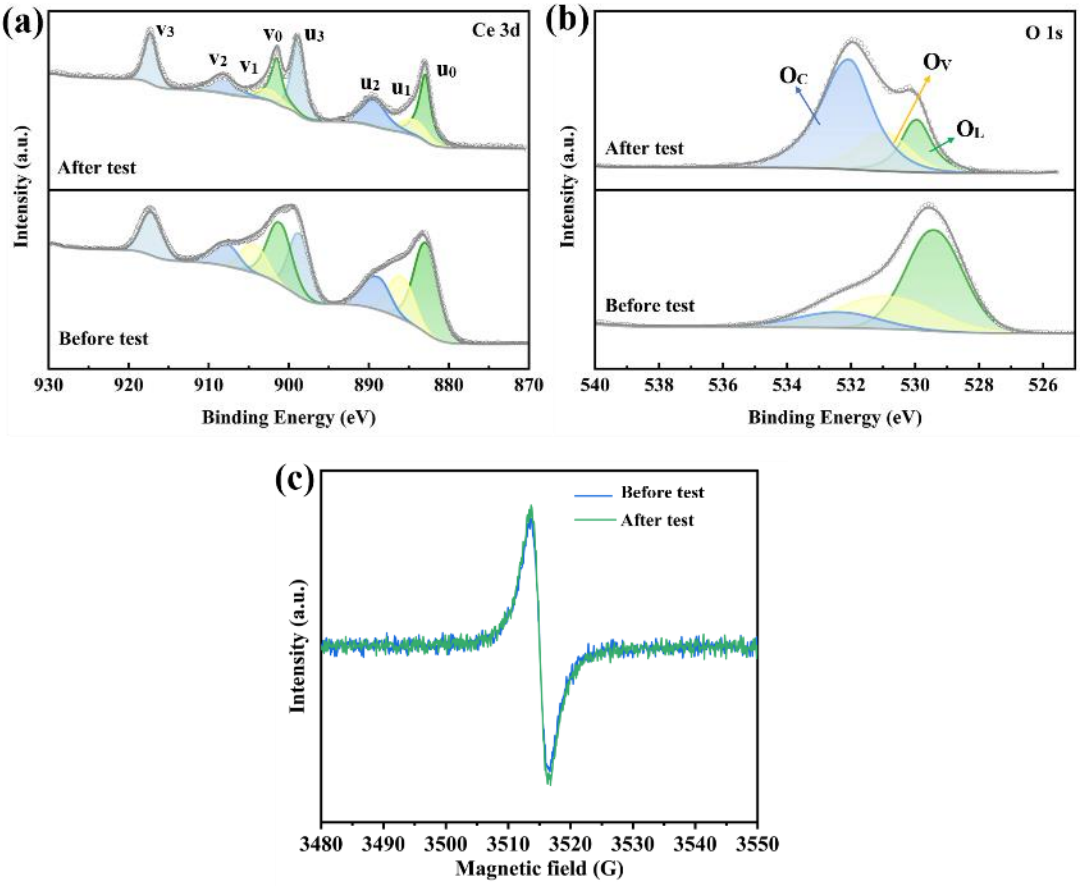

Figure S9. (a) XPS Ce 3d, (b) O 1s and (c) EPR spectra of CeO2-CTAB2.0 at before and after testing.

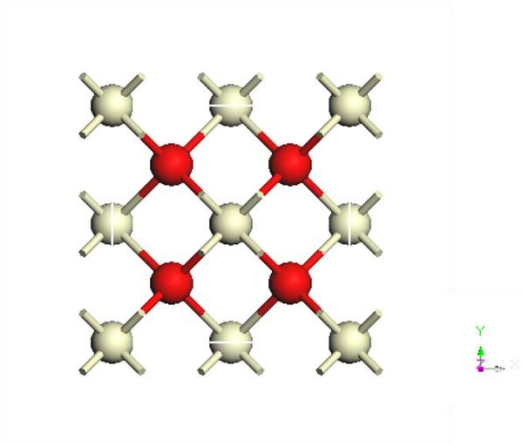

Figure S10. Atomic structure of CeO_2.

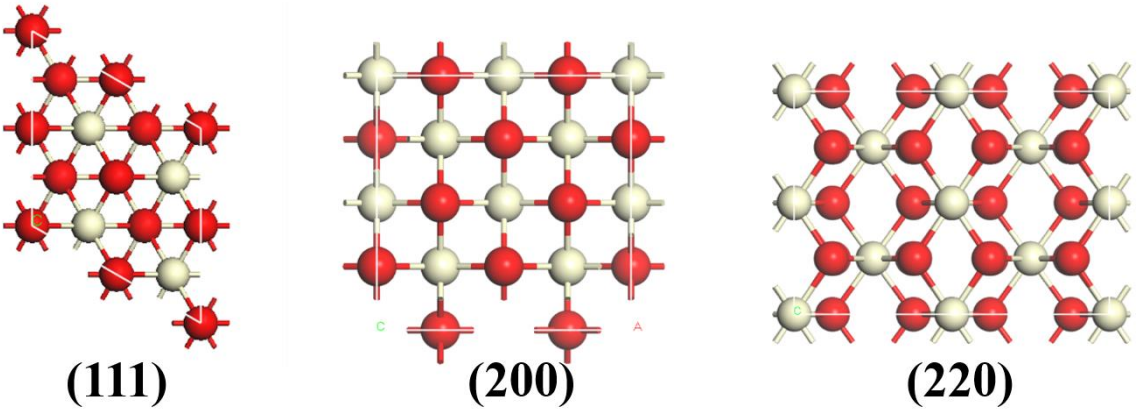

Figure S11. Atomic structure of CeO_2 (111), CeO_2 (200) and CeO_2 (220) slab models.

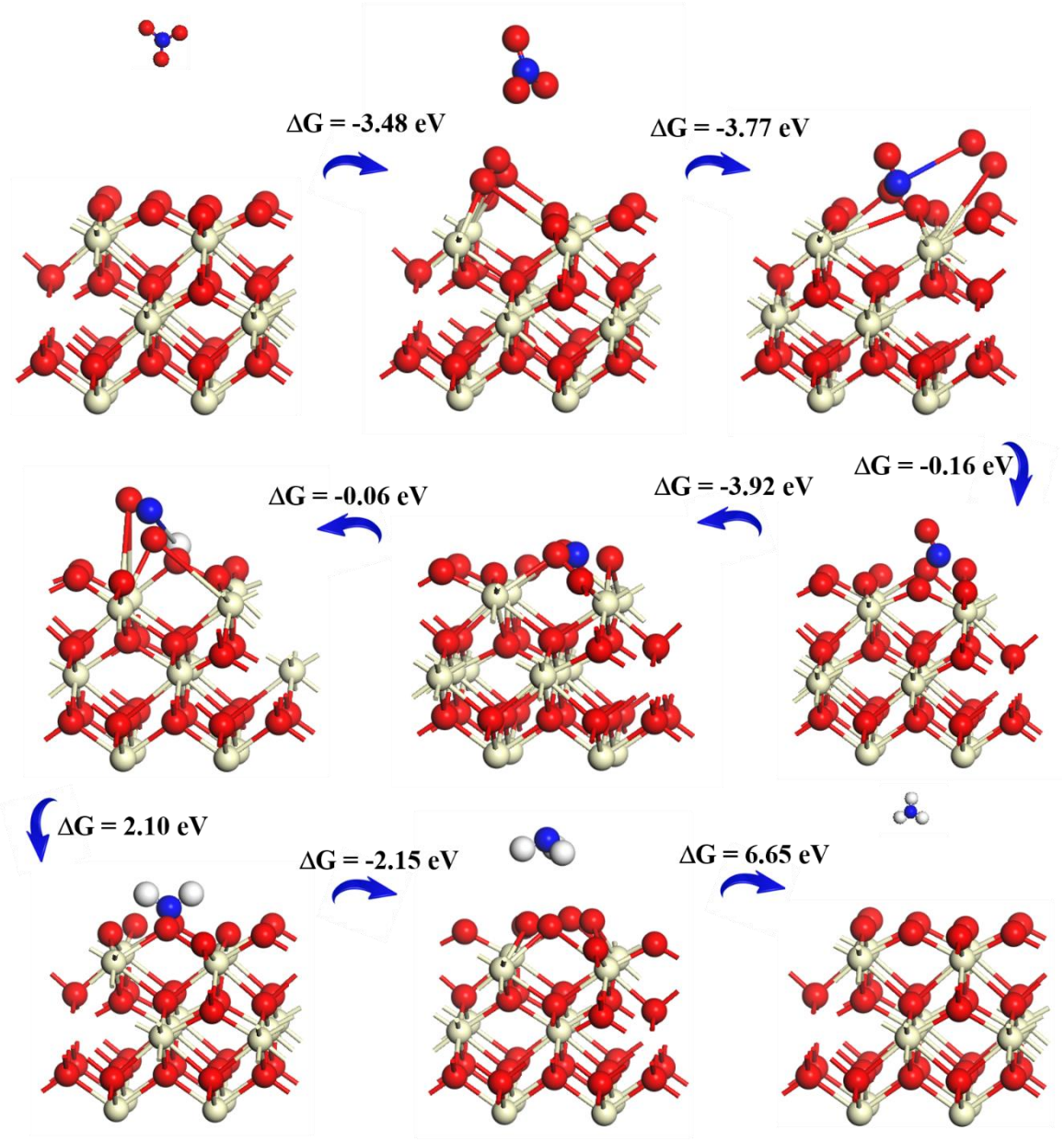

Figure S12. The optimized configurations of intermediates and corresponding free energy change involved in NO_3^- reduction on CeO_2 (200) surface.

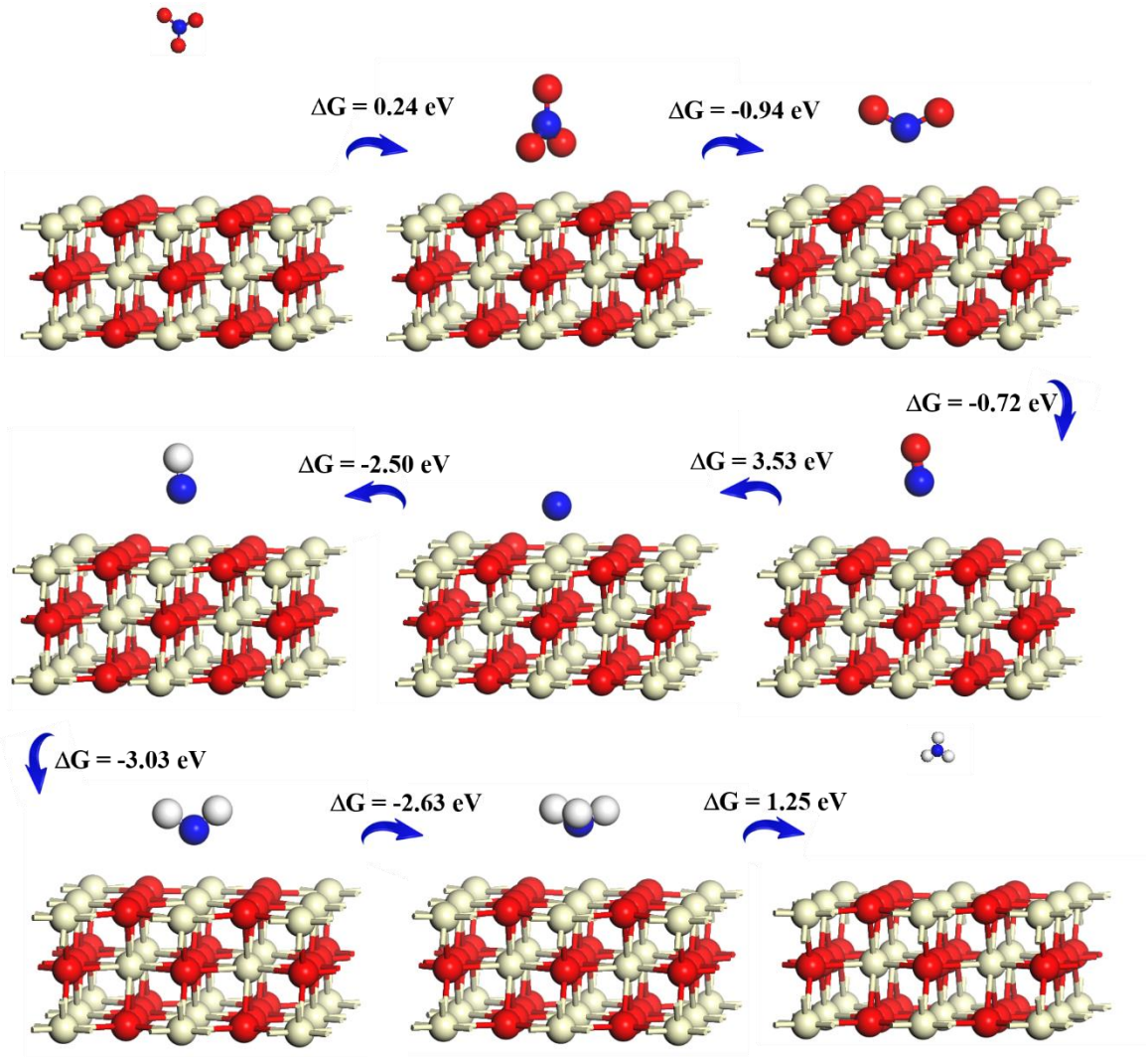

Figure S13. The optimized configurations of intermediates and corresponding free energy change involved in NO_3^- reduction on CeO_2 (220) surface.

References

[1] Wang Y, Zhang L, Niu Y, et al. Boosting NH_3 production from nitrate electroreduction via electronic structure engineering of Fe_3C nanoflakes. Green Chemistry 2021,23:7594-608.

[2] Xie H, Geng Q, Li X, et al. Ceria-reduced graphene oxide nanocomposite as an efficient electrocatalyst towards artificial N_2 conversion to NH_3 under ambient conditions. Chemical Communications 2019,55:10717-20.

[3] Gao E, Feng W, Jin Q, Han L, He Y. Exploring the effects of potassium-doping on the reactive oxygen species of CeO_2 (110) for formaldehyde catalytic oxidation: A DFT study. Surface Science 2024,740:122415.

[4] Vanpoucke D, Bultinck P, Cottenier S, Van Speybroeck V, Van Driessche I. Aliovalent doping of CeO_2: DFT study of oxidation state and vacancy effects. Journal of Materials Chemistry A 2014,2:13723-37.

[5] Castleton CW, Lee A, Kullgren J. Benchmarking density functional theory functionals for polarons in

oxides: properties of CeO_2. The Journal of Physical Chemistry C 2019,123:5164-75.
[6] Shi S, Tang Y, Ouyang C, et al. O-vacancy and surface on CeO_2: a first-principles study. Journal of Physics Chemistry of Solids 2010,71:788-96.
[7] Chen H, Huang H, Li H, et al. Self-Supporting Co/CeO_2 heterostructures for ampere-level current density alkaline water electrolysis. Inorganic Chemistry 2023,62:3297-304.
[8] Zhang Y, Chen X, Wang W, Yin L, Crittenden J. Electrocatalytic nitrate reduction to ammonia on defective Au_1Cu (111) single-atom alloys. Applied Catalysis B-Environmental 2022,310:121346.
[9] Shen Z, Yan J, Wang M, et al. Cu/Cu^+ synergetic effect in Cu_2O/Cu/CF electrocatalysts for efficient nitrate reduction to ammonia. ACS Sustainable Chemistry & Engineering 2023,11:9433-41.
[10] Wang Y, Zhou W, Jia R, Yu Y, Zhang B. Unveiling the activity origin of a copper-based electrocatalyst for selective nitrate reduction to ammonia. Angewandte Chemie-International Edition 2020,59:5350-4.